Maynooth Wave Energy Workshop 2026

Realistic energy-maximising control of cyclorotor wave energy converters using estimator, predictor, and nonlinear MPC.

MaxRotorWEC project

Ilias Stasinopoulos[1], A. Ermakov[1], J.V. Ringwood[1].

January 23, 2026

[1]Centre for Ocean Energy Research, National University of Ireland Maynooth.

Presentation outline

1. Introduction
2. Mathematical model
3. Performance metric
4. Realistic control system for a cyclorotor WEC
5. Results
6. Conclusions and discussion

Introduction

The cyclorotor WEC

The **cyclorotor** is a relatively new direction for **Wave Energy Converters (WECs)**, which obtains energy from the generation of significant lift forces on rotating hydrofoils caused by the elliptical motion of water particles.

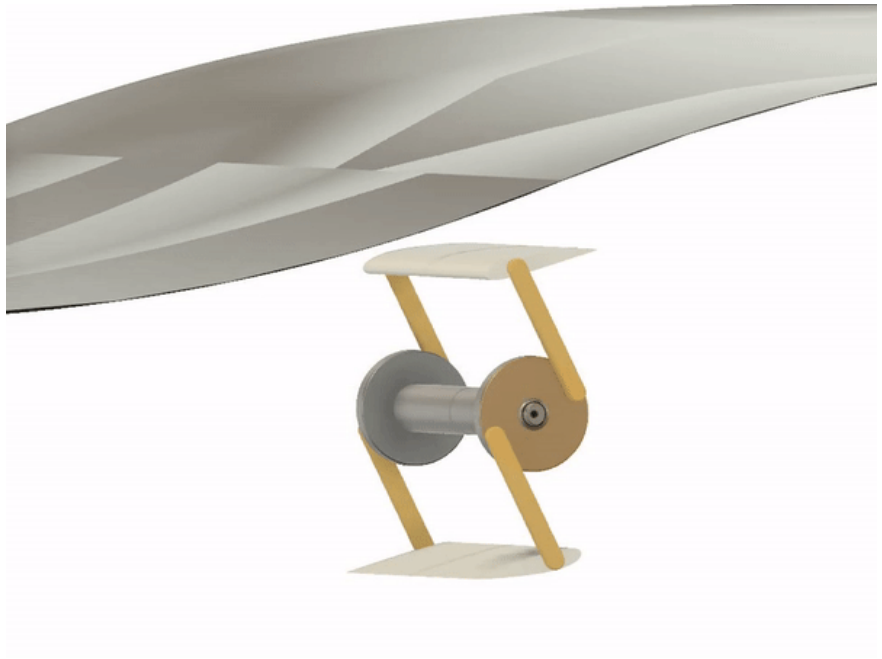

The cyclorotor WEC

Appealing characteristics:

- Greater power production potential: 70% or more of the power available in an irregular wave
- Unidirectional rotation
- Storm survival

The cyclorotor WEC

Appealing characteristics:

- Greater power production potential: 70% or more of the power available in an irregular wave
- Unidirectional rotation
- Storm survival

Challenges:

- Complex hydrodynamics effects
- High nonlinearity of the models

Experimental setup 3D tests

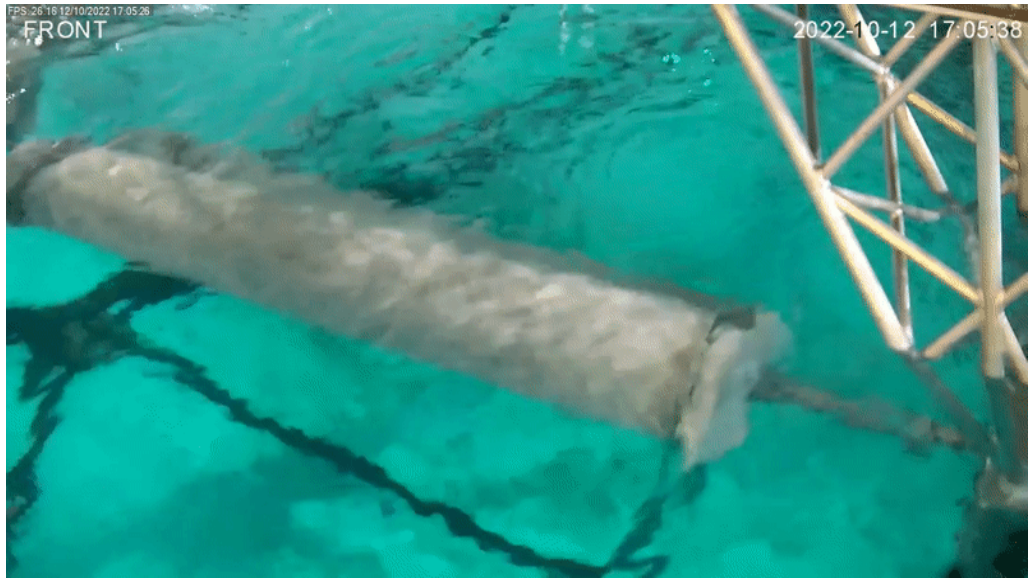

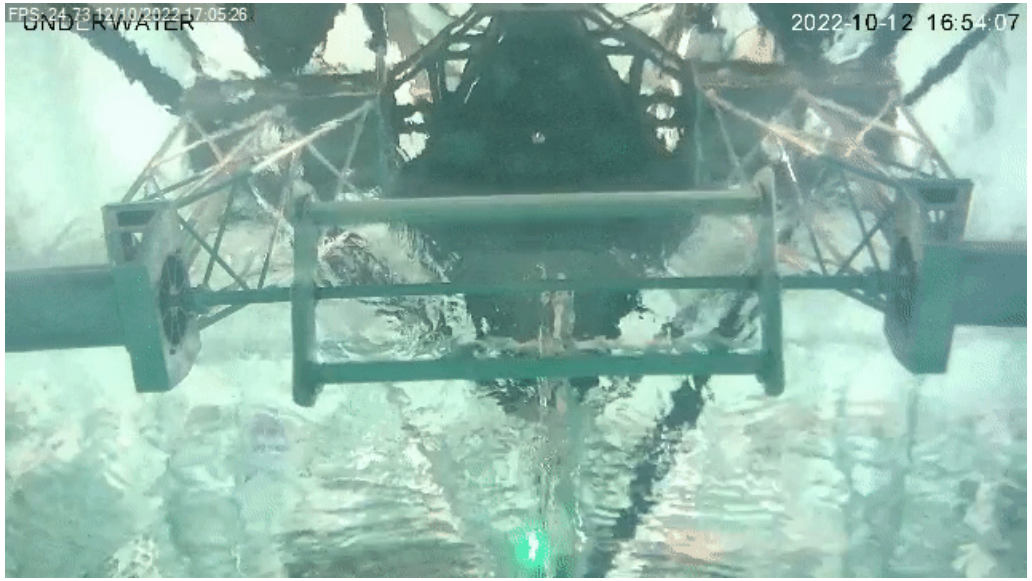

MaxRotorWEC project

The overall aim of the **MaxRotorWEC** project is to provide technical and economic solutions to the existing problems faced in the design of a radically new wave energy converter concept that exploits hydrodynamic lift forces and can bring wave energy to commercial fruition in the form of a new real-time control strategy.

Selected approach

Monochromatic waves

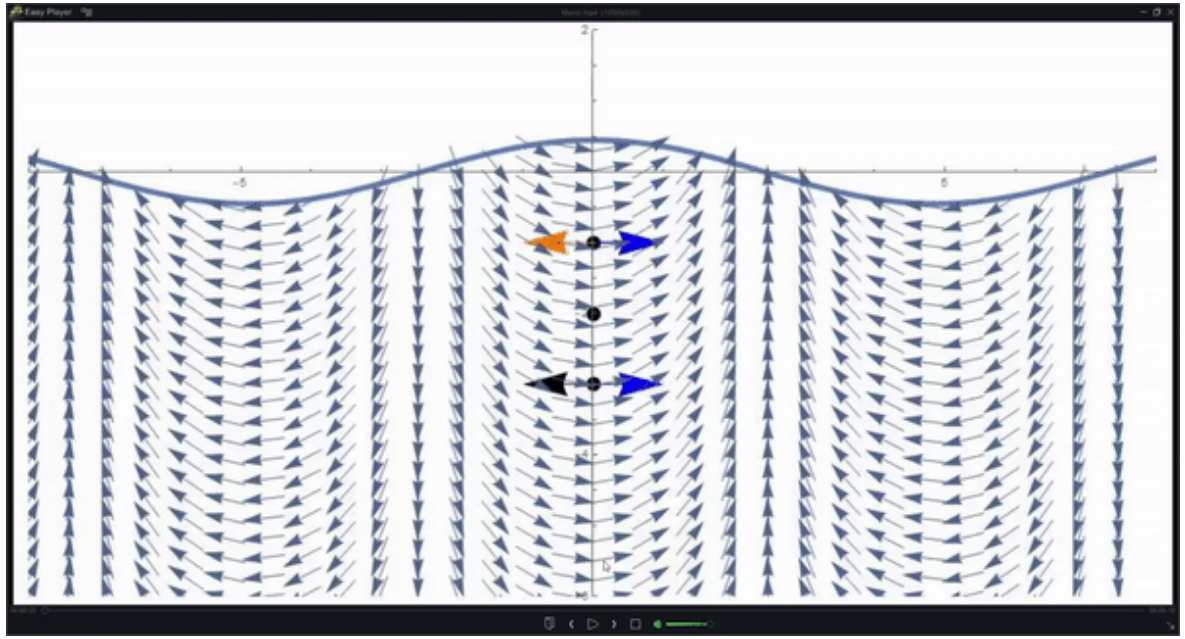

Panchromatic waves

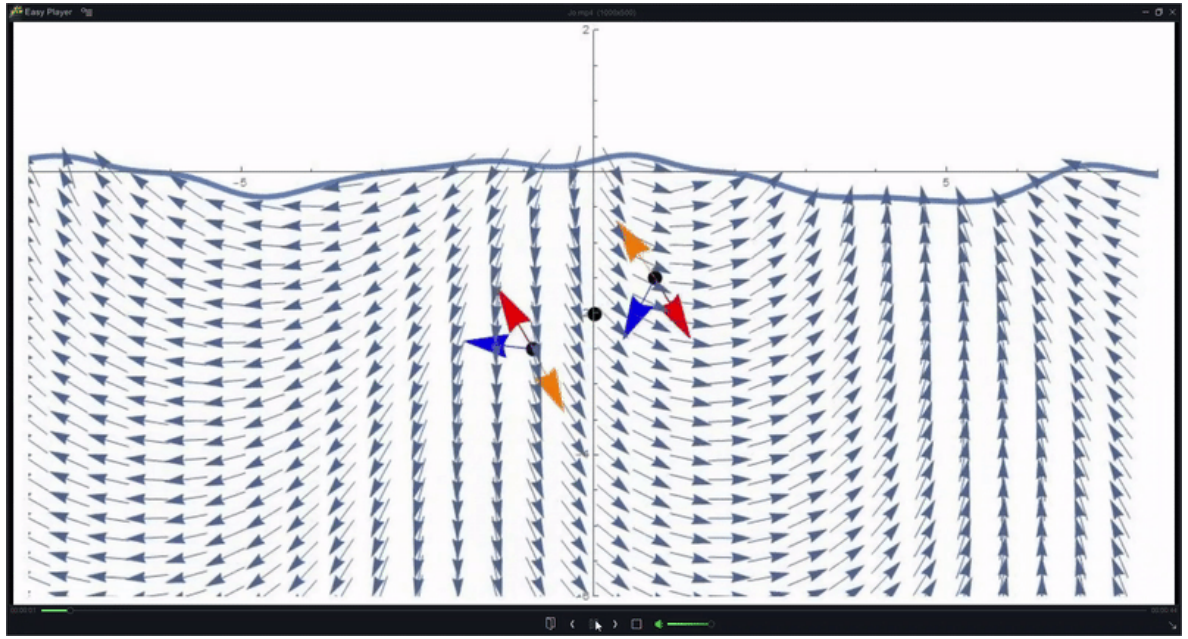

Black arrow shows the direction of the rotation, red arrow shows the direction of the tangential force, blue arrow the direction of wave radiated by the foils, orange arrow the direction of the drag force.

Selected approach

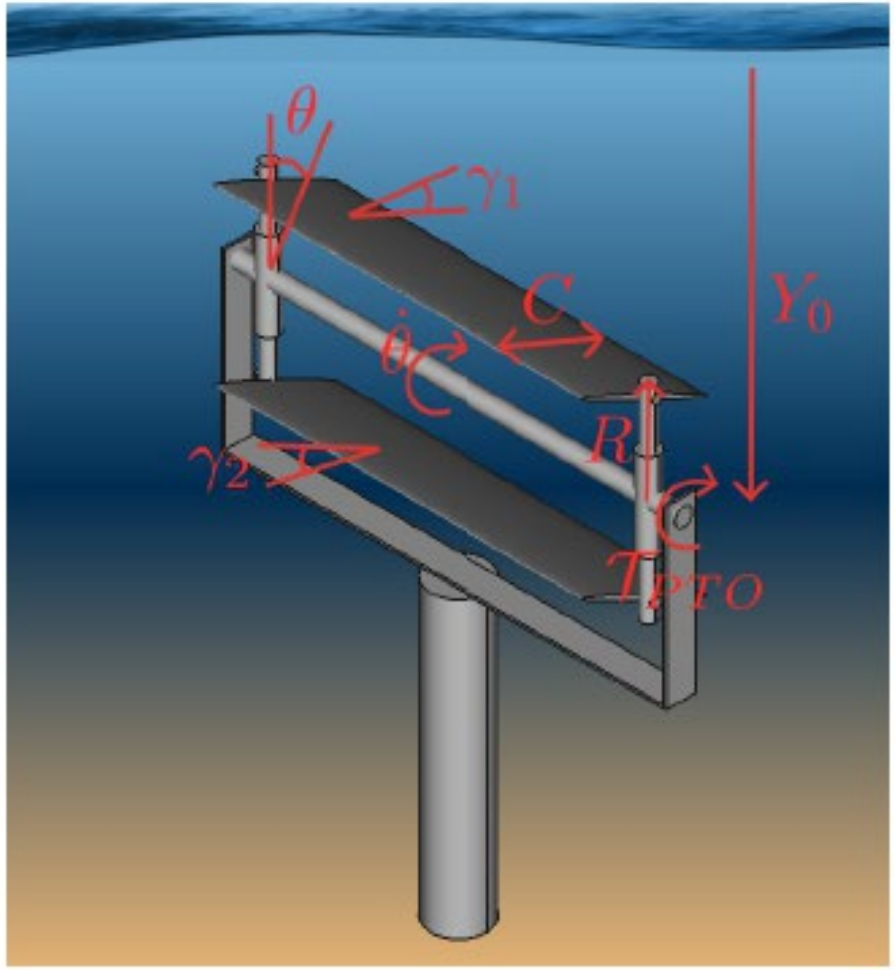

Figure 1: Concept of a twin-foil cyclorotor WEC, illustrating key structural parameters and control actuators.

- Cyclorotor WECs offer a variety of structural parameters and potential control actuators:

Structural parameters: rotor radius R, hydrofoil chord length C.

Selected approach

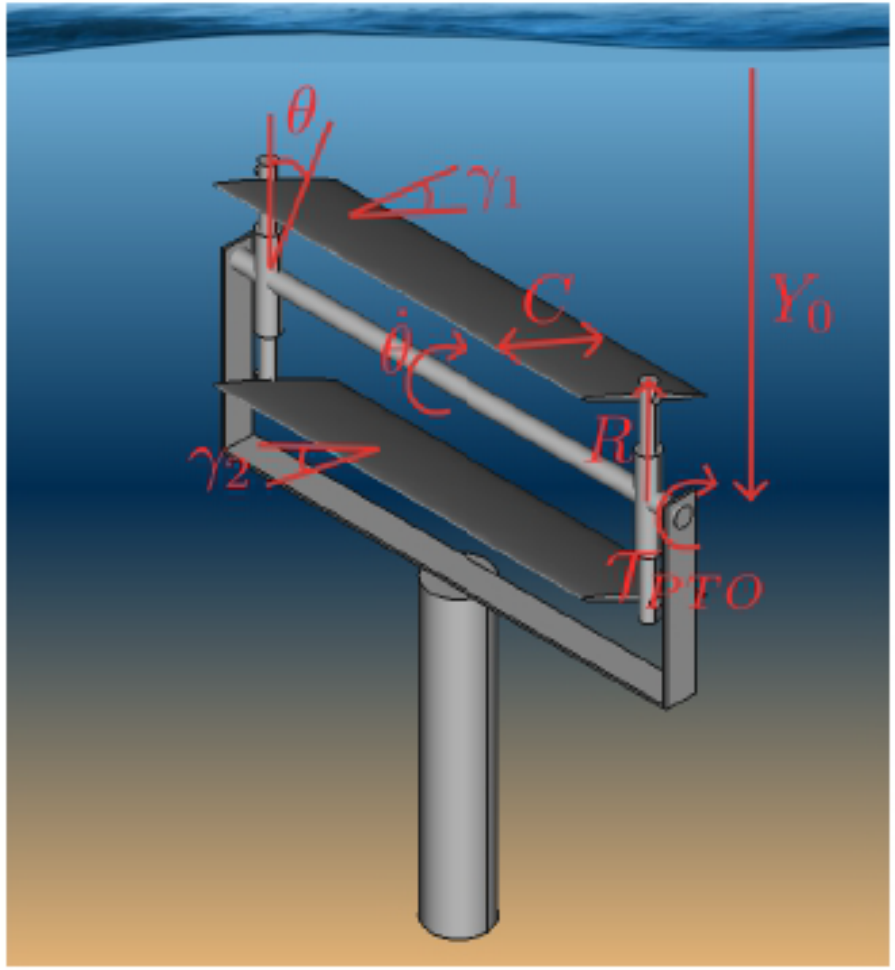

Figure 1: Concept of a twin-foil cyclorotor WEC, illustrating key structural parameters and control actuators.

- Cyclorotor WECs offer a variety of structural parameters and potential control actuators:

Structural parameters: rotor radius R, hydrofoil chord length C.

Slow control inputs: submergence depth Y_0.

Selected approach

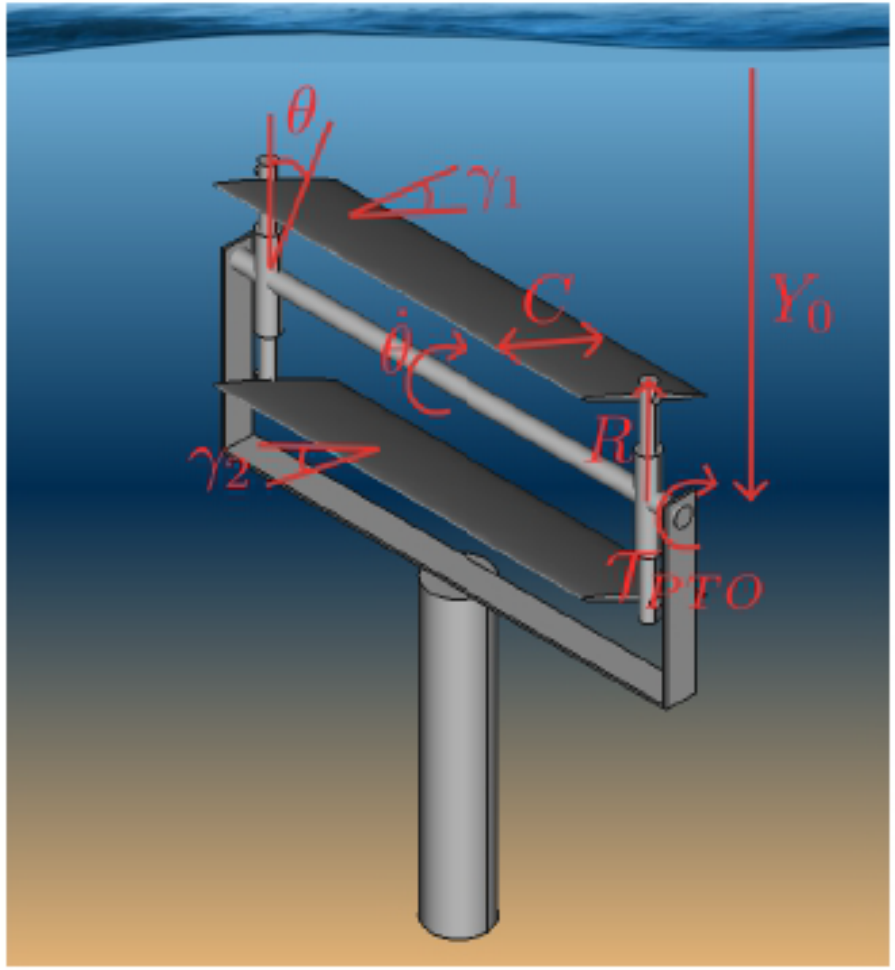

Figure 1: Concept of a twin-foil cyclorotor WEC, illustrating key structural parameters and control actuators.

- Cyclorotor WECs offer a variety of structural parameters and potential control actuators:

Structural parameters: rotor radius R, hydrofoil chord length C.

Slow control inputs: submergence depth Y_0.

Fast real time control inputs: hydrofoil pitch angles γ_1, γ_2, and PTO torque $\mathcal{T}_{PTO}$, used to regulate rotational velocity $\dot{\theta}$.

- The latter variables are particularly critical for maximizing power production.

Motivation and contribution

- Most numerical performance evaluations are carried out in (relatively unrealistic) regular wave conditions or in short-duration simulations of irregular waves (< 10 min).

Motivation and contribution

- Most numerical performance evaluations are carried out in (relatively unrealistic) regular wave conditions or in short-duration simulations of irregular waves (< 10 min).

- Tested control strategies assume perfect knowledge of the relative foil-fluid velocity, and therefore do not account for potential losses from estimation and prediction errors.

Motivation and contribution

- Most numerical performance evaluations are carried out in (relatively unrealistic) regular wave conditions or in short-duration simulations of irregular waves (< 10 min).

- Tested control strategies assume perfect knowledge of the relative foil-fluid velocity, and therefore do not account for potential losses from estimation and prediction errors.

Main contribution

This work introduces **the first realistic energy-maximising control system for a cyclorotor WEC, integrating an estimator and a predictor** of the relative foil-fluid velocity in irregular waves, together with a Nonlinear Model Predictive Control (NMPC) approach.

Motivation and contribution

- This estimator-predictor-NMPC structure is fundamentally different from existing control formulations for traditional WECs:
  - Severe nonlinearity of mathematical models.
  - Rapidly changing relative foil-fluid velocity as the system input.
  - Multiple control inputs and diverse set of sensors.

Motivation and contribution

▶ This estimator-predictor-NMPC structure is fundamentally different from existing control formulations for traditional WECs:

- Severe nonlinearity of mathematical models.
- Rapidly changing relative foil-fluid velocity as the system input.
- Multiple control inputs and diverse set of sensors.

Other contributions

▶ The reduction in energy capture due to the inaccuracies in estimation and prediction is quantified.

Motivation and contribution

▶ This estimator-predictor-NMPC structure is fundamentally different from existing control formulations for traditional WECs:

- Severe nonlinearity of mathematical models.
- Rapidly changing relative foil-fluid velocity as the system input.
- Multiple control inputs and diverse set of sensors.

Other contributions

▶ The reduction in energy capture due to the inaccuracies in estimation and prediction is quantified.

▶ A comparison between realistic and idealized control is conducted for two ocean regions, in terms of annual power output.

Mathematical model

Mathematical model

A 2-D control-oriented mathematical model is used [1] .

Position:

$$x_i(t) = R\cos\left(\theta(t) + \pi(i-1)\right),$$
$$y_i(t) = Y_0 - R\sin\left(\theta(t) + \pi(i-1)\right),$$

[1] A. Ermakov, F. Thiebaut, G. S. Payne, and J. V. Ringwood, "Validation of a control-oriented point vortex model for a cyclorotor-based wave energy device," *J. Fluids Struct.*, vol. 119, p. 103875, 2023.

Mathematical model

A 2-D control-oriented mathematical model is used [1] .

Position:

$$x_i(t) = R\cos\left(\theta(t) + \pi(i-1)\right),$$
$$y_i(t) = Y_0 - R\sin\left(\theta(t) + \pi(i-1)\right),$$

Rotational velocity:

$$(V_{R_i})_x(t) = -R\dot{\theta}\sin\left(\theta(t) + \pi(i-1)\right),$$
$$(V_{R_i})_y(t) = -R\dot{\theta}\cos\left(\theta(t) + \pi(i-1)\right),$$

where $i = 1, 2$ is the hydrofoil number, $\theta(t)$ represents the angular position of the rotor in polar coordinates, $\dot{\theta}(t)$ is the angular velocity, R is the rotor radius, and Y_0 is the submergence depth of the rotor center.

[1] A. Ermakov, F. Thiebaut, G. S. Payne, and J. V. Ringwood, "Validation of a control-oriented point vortex model for a cyclorotor-based wave energy device," *J. Fluids Struct.*, vol. 119, p. 103875, 2023.

Mathematical model

The **relative foil-fluid velocity** is defined as the vector difference between the local wave-induced fluid velocity V_W (modeled with JONSWAP spectrum)[2] and the hydrofoil rotational velocity V_R, augmented by the additional contribution from wake-induced and radiative effects V_H (modeled using a complex potential formulation)[3]:

$$\hat{\mathbf{V}}_\mathbf{i} = \mathbf{V}_{\mathbf{W}_\mathbf{i}} - \mathbf{V}_{\mathbf{R}_\mathbf{i}} + \mathbf{V}_{\mathbf{H}_\mathbf{i}}\,.$$

[2] A. Arredondo-Galeana, A. Ermakov, W. Shi, J. V. Ringwood, and F. Brennan, "Optimal control of wave cycloidal rotors with passively morphing foils: An analytical and numerical study," *Mar. Struct.*, vol. 95, p. 103597, 2024.

[3] A. Ermakov, F. Thiebaut, G. S. Payne, and J. V. Ringwood, "Validation of a control-oriented point vortex model for a cyclorotor-based wave energy device," *J. Fluids Struct.*, vol. 119, p. 103875, 2023.

The **angle of attack** for each hydrofoil is calculated as:

$$\alpha_i(t) = \arcsin\left(\frac{(V_{R_i})_x * (\hat{V}_i)_y - (V_{R_i})_y * (\hat{V}_i)_x}{|V_{R_i}||\hat{V}_i|}\right) + \gamma_i,$$

where γ_i is the pitch angle of hydrofoil i.

The **angle of attack** for each hydrofoil is calculated as:

$$\alpha_i(t) = \arcsin\left(\frac{(V_{R_i})_x * (\hat{V}_i)_y - (V_{R_i})_y * (\hat{V}_i)_x}{|V_{R_i}||\hat{V}_i|}\right) + \gamma_i,$$

where γ_i is the pitch angle of hydrofoil i.

Then, the **lift and drag forces** acting on the rotating hydrofoils can be evaluated as:

$$F_{L_i} = \frac{1}{2} C\, C_L(a_i)|\hat{V}_i|^2, \quad F_{D_i} = \frac{1}{2} C\, C_D(a_i)|\hat{V}_i|^2,$$

where C is the hydrofoil chord length, C_L and C_D are the lift and drag coefficients, respectively, which are functions of the angle of attack a_i.

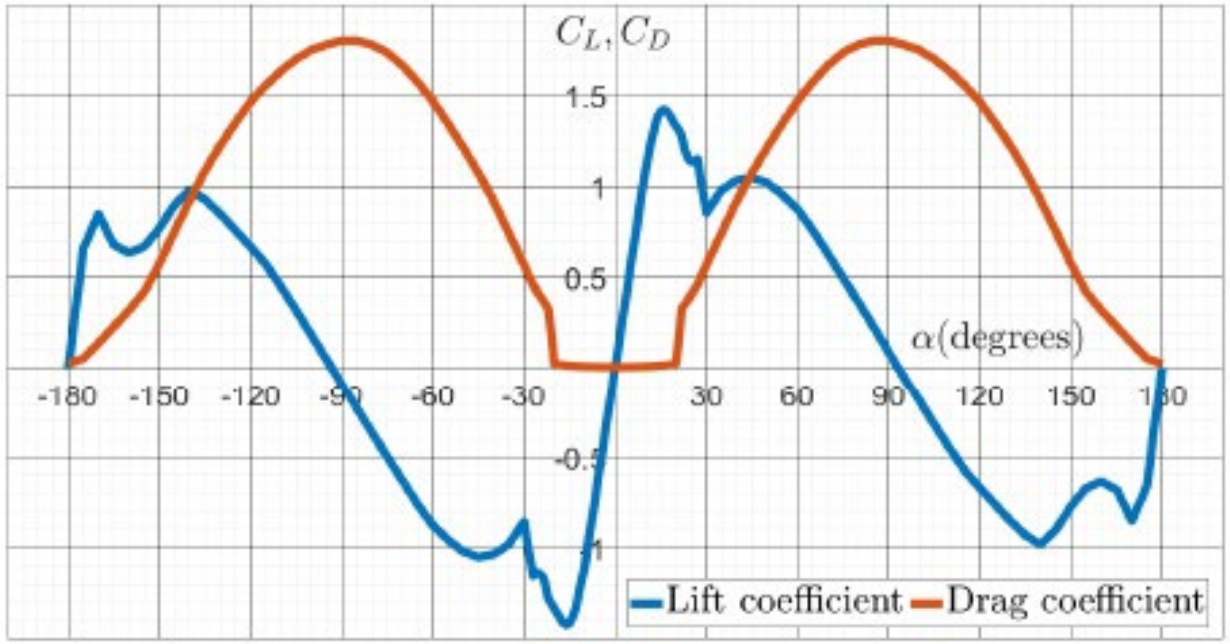

Figure 2: Lift and drag coefficients for NACA0015 hydrofoil for Reynolds numbers in the range $10^4 \leq Re \leq 10^7$.

Mathematical model

The **tangential and radial forces** on each hydrofoil i are obtained by projecting the lift and drag forces along the tangential and radial directions of the hydrofoil circular trajectory:

$$F_{T_i} = F_{L_i} \sin(\alpha_i - \gamma_i) - F_{D_i} \cos(\alpha_i - \gamma_i),$$
$$F_{R_i} = F_{L_i} \cos(\alpha_i - \gamma_i) + F_{D_i} \sin(\alpha_i - \gamma_i).$$

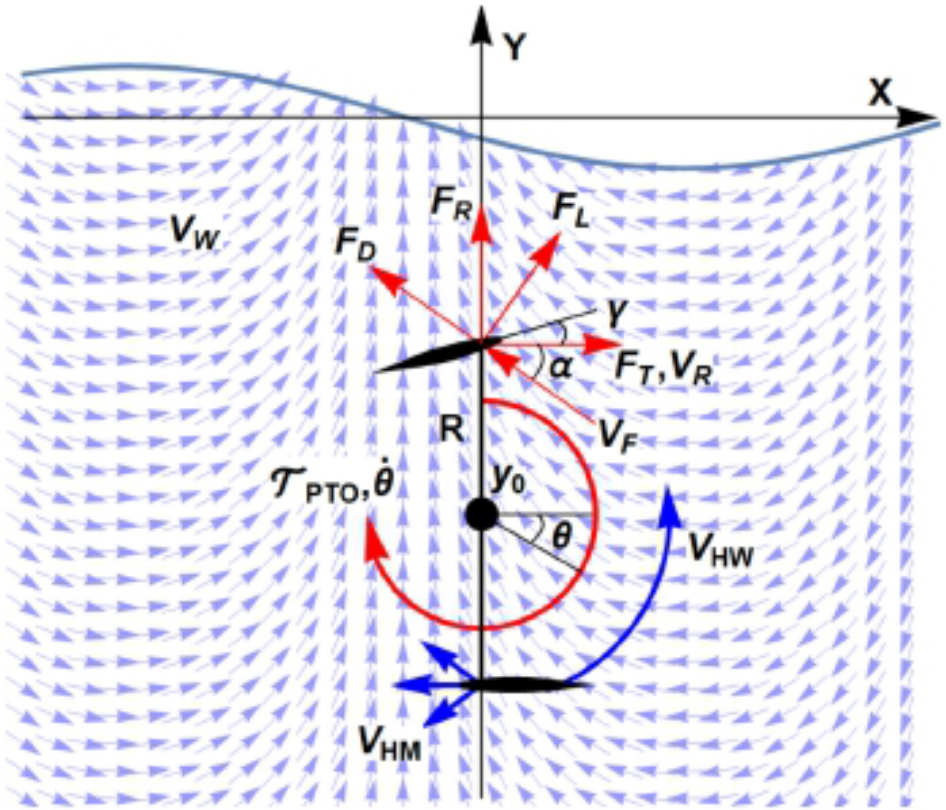

Figure 3: Two-dimensional mathematical model illustrating the operating principle of a cyclorotor WEC.

Mathematical model

The tangential components of the lift and drag forces accelerate or decelerate the cyclorotor rotation, generating the wave-induced torque $\mathcal{T}_{Wave}$, which is evaluated as:

$$\mathcal{T}_{Wave} = (F_{T_1} + F_{T_2})R.$$

Mathematical model

The tangential components of the lift and drag forces accelerate or decelerate the cyclorotor rotation, generating the wave-induced torque $\mathcal{T}_{Wave}$, which is evaluated as:

$$\mathcal{T}_{Wave} = (F_{T_1} + F_{T_2})R.$$

Wave power is extracted by applying a power take-off (PTO) torque, $\mathcal{T}_{PTO}$. As a result, the dynamics of the controlled cyclorotor are governed by Newton's second law of rotation:

$$I\ddot{\theta}(t) = \mathcal{T}_{Wave} - \mathcal{T}_{PTO},$$

where I is the inertia of the rotor, $\ddot{\theta}$ is the angular acceleration.

Performance metric

Performance metric

Mechanical power: The time-averaged mechanical shaft power generated by the cyclorotor WEC over the time interval $[0, T_0]$ is defined as the product of the rotational velocity $\dot{\theta}$ and the applied PTO torque $\mathcal{T}_{PTO}$.

$$\bar{P}_{Shaft} = \frac{1}{T_0} \int_0^{T_0} \mathcal{T}_{PTO} \dot{\theta}(t)\, dt.$$

Performance metric

Mechanical power: The time-averaged mechanical shaft power generated by the cyclorotor WEC over the time interval $[0, T_0]$ is defined as the product of the rotational velocity $\dot{\theta}$ and the applied PTO torque $\mathcal{T}_{PTO}$.

$$\bar{P}_{Shaft} = \frac{1}{T_0} \int_0^{T_0} \mathcal{T}_{PTO} \dot{\theta}(t)\, dt.$$

Performance function

$$J = \frac{1}{T_0} \int_0^{T_0} \left(\mathcal{T}_{PTO} \dot{\theta} - \mu \Delta \mathcal{T}_{PTO}^2 \right) dt,$$

where μ is a tunable weighting factor that penalizes large fluctuations in the PTO torque, and $\Delta \mathcal{T}_{PTO}$ denotes the maximum variation in PTO torque observed over the time interval T_0.

Performance metric

An additional post-processing metric to evaluate the efficiency of wave energy conversion is the **Capture Width Ratio (CWR)**:

$$CWR = \frac{\bar{P}_{Shaft}}{P_{Wave}} \times 100\%,$$

where P_{Wave} is the power available for absorption in an irregular wave.

Performance metric

An additional post-processing metric to evaluate the efficiency of wave energy conversion is the **Capture Width Ratio (CWR)**:

$$CWR = \frac{\bar{P}_{Shaft}}{P_{Wave}} \times 100\%,$$

where P_{Wave} is the power available for absorption in an irregular wave.

The **total annual mechanical energy production** in a coastal location is calculated using the following expression. It sums the product of the time-averaged power output for each sea state, $\bar{P}_{Shaft}(H_s, T_p)$, its **probability of occurrence**, $p(H_s, T_p)$, and the total number of seconds in a year, $T_{seconds}$:

$$P_{Annual} = \sum^{T_p} \sum^{H_s} \bar{P}_{Shaft}(H_s, T_p) \cdot p(H_s, T_p) \cdot T_{seconds}.$$

Sea locations

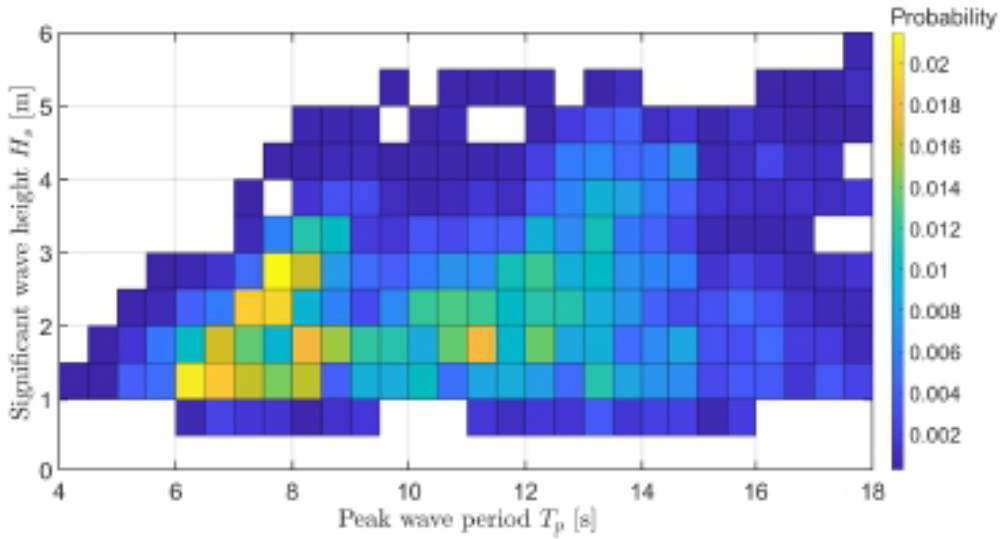

(a) Humboldt Bay, located off the US West Coast (California).

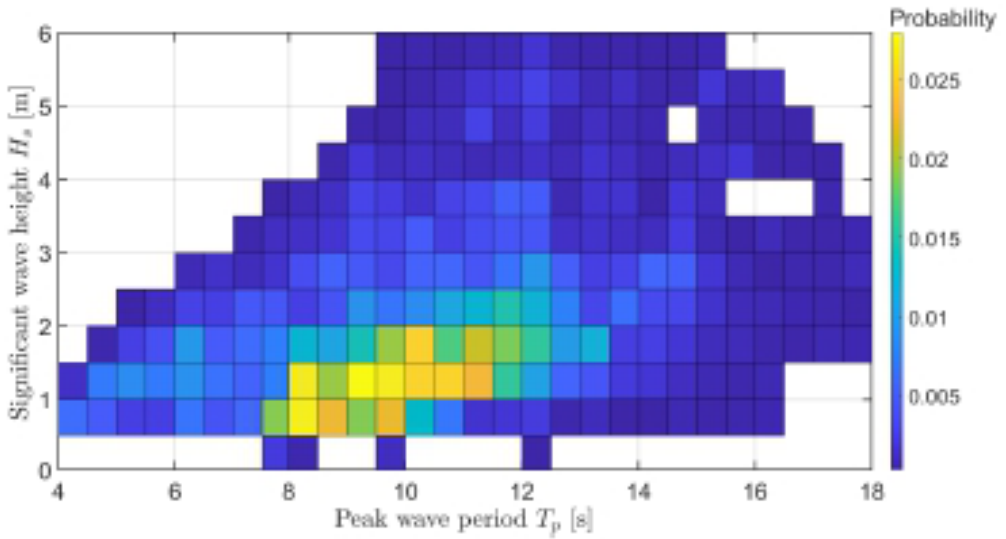

(b) Bay of Biscay, located off the North Atlantic coast of France.

Figure 4: Scatter plots of the probability distribution of different sea state occurrences at two locations, for the year 2024. The data were obtained from the ERA5 dataset [4].

[4] ECMWF, 2025. European centre for medium-range weather forecasts. www.copernicus.eu/en. [Accessed 26-05-2025]

Realistic control system for a cyclorotor WEC

Control architecture: The grand plan!

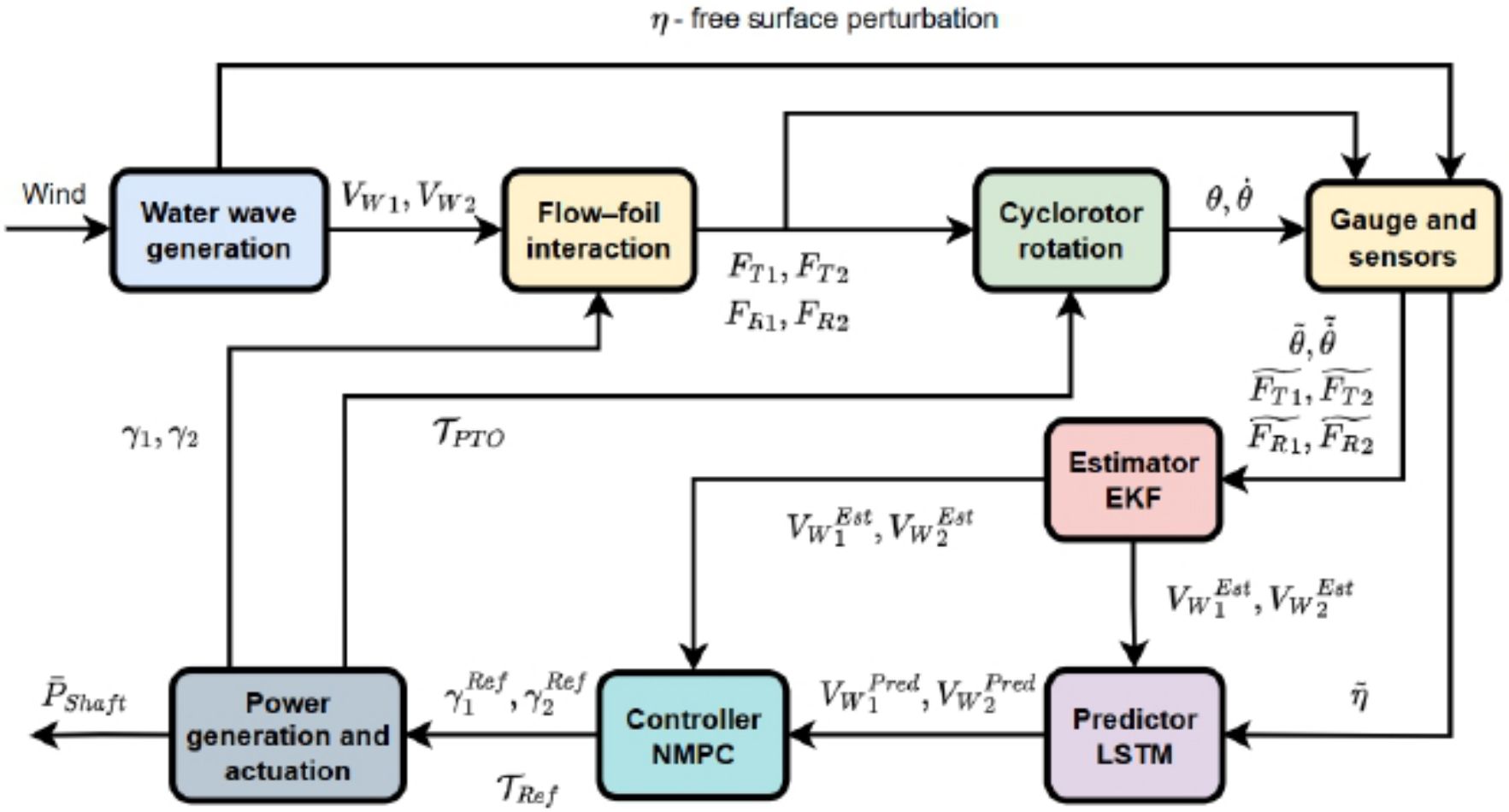

Figure 5: Diagram of the proposed realistic control architecture for a cyclorotor WEC.

Estimator

The wave-induced fluid velocity is estimated using the **Extended Kalman Filter (EKF)**, which incoporates measurements of tangential and radial forces from sensors mounted on the hydrofoils, along with rotational velocity measurements from sensors located on the rotor shaft[5].

The relative foil/fluid velocity is reconstructed via: $\hat{\mathbf{V}} = \mathbf{V_W} - \mathbf{V_R} + \mathbf{V_H}$.

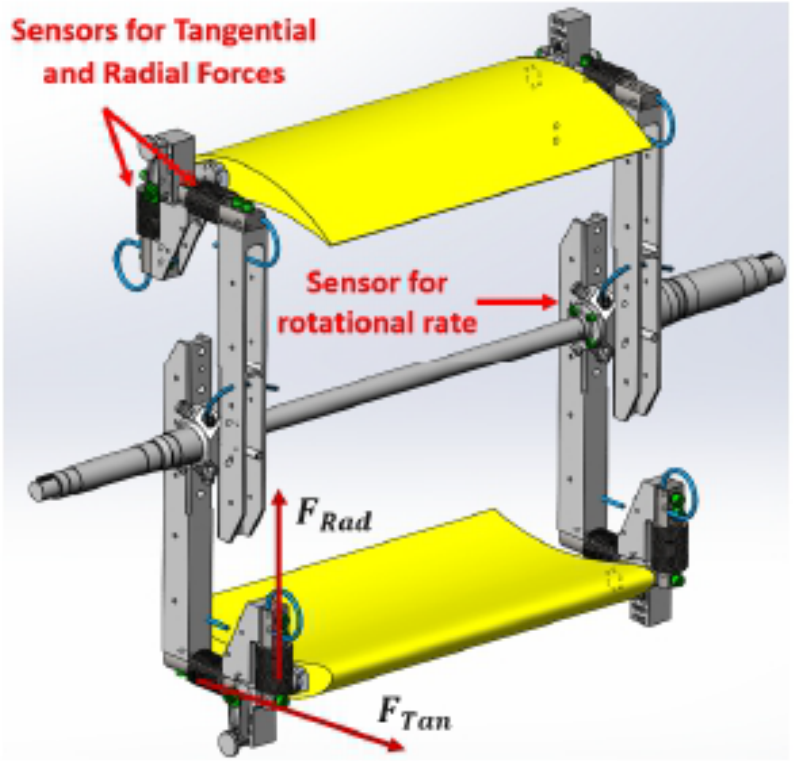

Figure 6: Sensors system for cyclorotor based WEC.

[5] I. Stasinopoulos, A. M. Ermakov, and J. V. Ringwood, "Relative foil-fluid velocity estimation and forecasting for cyclorotor wave energy conversion," in *Proc. IEEE OCEANS 2025 Conf.*, Brest, France, 2025.

Estimator

The dynamics of the cyclorotor are governed by Newton's second law of rotation. The control-oriented mathematical model described before is employed:

$$\ddot{\theta} = \frac{\left(F_{T_1}(\gamma_1, \dot{\theta}, V_{W_1}) + F_{T_2}(\gamma_2, \dot{\theta}, V_{W_2})\right) R - \mathcal{T}_{PTO}}{I}.$$

Table 1: Estimator parameters

Measurable variables:	$\widetilde{\dot{\theta}}, \widetilde{F_{T_1}}, \widetilde{F_{R_1}}, \widetilde{F_{T_2}}, \widetilde{F_{R_2}}$
Estimated variables:	$\dot{\theta}^{Est}, (V_{W_1}^{Est})_x, (V_{W_1}^{Est})_y, (V_{W_2}^{Est})_x, (V_{W_2}^{Est})_y$
Constants:	R, I
Other variables:	$\ddot{\theta}$
Control inputs:	$\gamma_1, \gamma_2, \mathcal{T}_{PTO}$

Figure 7: Cyclorotor WEC concept suggested by the Atargis Energy Corporation.

- The Extended Kalman Filter is implemented in MATLAB and tested on a cyclorotor similar to the one suggested by the Atargis Energy Corporation[5].

[5] S. G. Siegel, "Numerical benchmarking study of a cycloidal wave energy converter," *Renew. Energy*, vol. 134, pp. 390–405, 2019.

Figure 7: Cyclorotor WEC concept suggested by the Atargis Energy Corporation.

- The Extended Kalman Filter is implemented in MATLAB and tested on a cyclorotor similar to the one suggested by the Atargis Energy Corporation[5].
- The cyclorotor has radius $R = 6\text{m}$, a submergence depth $Y_0 = -12\text{m}$ and is equipped with two hydrofoils NACA0015 with chord length $C = 5\text{m}$, and section mass $m = 1000\text{kg/m}$.

[5] S. G. Siegel, "Numerical benchmarking study of a cycloidal wave energy converter," *Renew. Energy*, vol. 134, pp. 390–405, 2019.

Figure 7: Cyclorotor WEC concept suggested by the Atargis Energy Corporation.

- The Extended Kalman Filter is implemented in MATLAB and tested on a cyclorotor similar to the one suggested by the Atargis Energy Corporation[5].
- The cyclorotor has radius $R = 6\text{m}$, a submergence depth $Y_0 = -12\text{m}$ and is equipped with two hydrofoils NACA0015 with chord length $C = 5\text{m}$, and section mass $m = 1000\text{kg/m}$.
- A panchromatic sea state with peak period $T_p = 10\text{s}$ and significant height $H_s = 2\text{m}$ is simulated.

[5] S. G. Siegel, "Numerical benchmarking study of a cycloidal wave energy converter," *Renew. Energy*, vol. 134, pp. 390–405, 2019.

Estimator

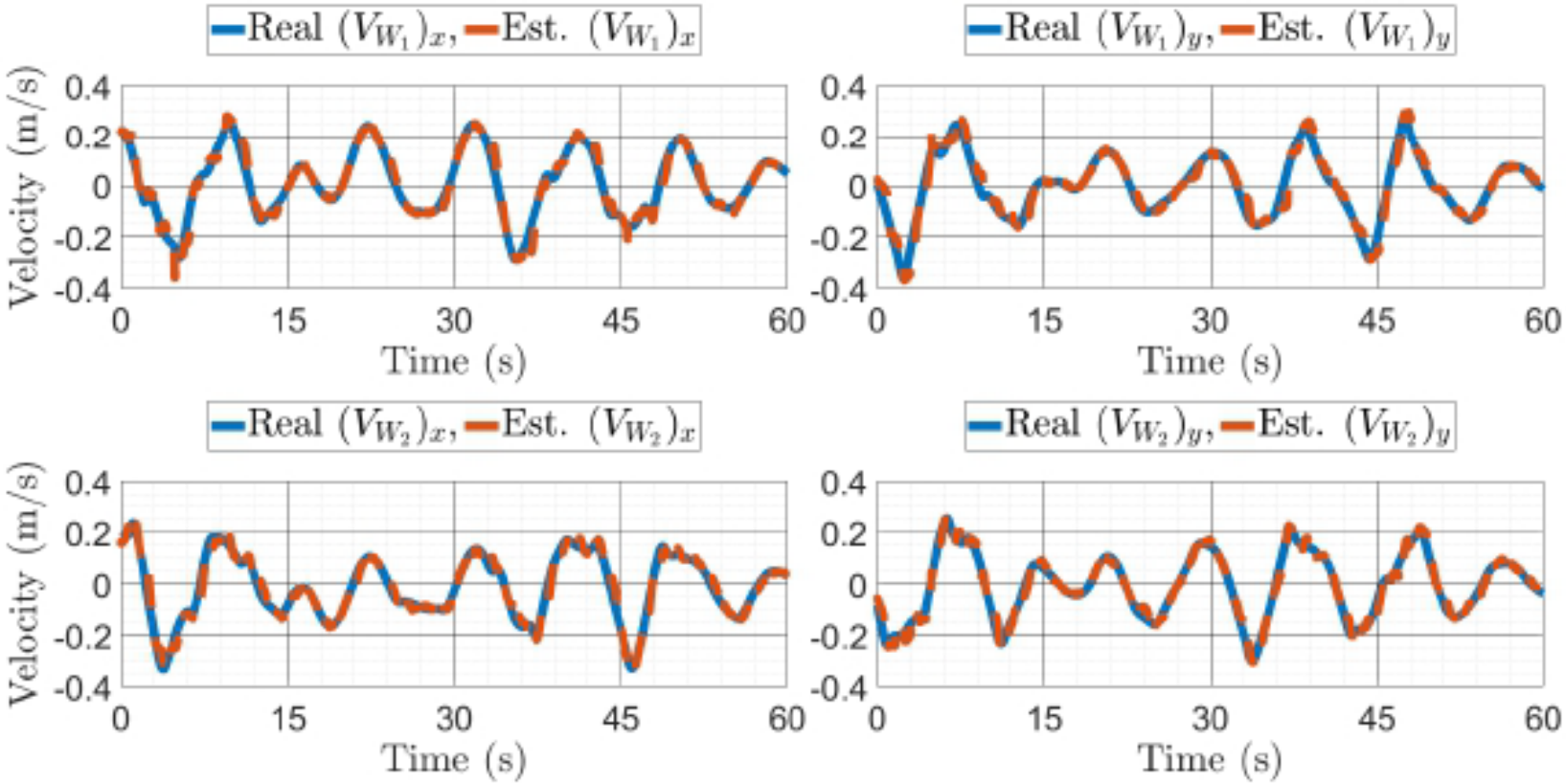

Figure 8: Comparison between the actual and estimated x and y components of the wave-induced fluid velocity vector $\mathbf{V_W}$ for both hydrofoils, assuming a 5% model error and a 10% sensor error.

Predictor

The predictor for the relative foil/fluid velocity is based on a **Long Short Term Memory (LSTM)** Recursive Neural Network (RNN)[6].

Inputs:

- Previously estimated values of wave-induced fluid velocity for hydrofoils.
- Measurements of free surface elevation a gauge located up-wave.

Outputs: Prediction of wave-induced fluid velocity. The relative foil/fluid velocity is reconstructed via: $\hat{\mathbf{V}} = \mathbf{V_W} - \mathbf{V_R} + \mathbf{V_H}$.

[6] I. Stasinopoulos, A. M. Ermakov, and J. V. Ringwood, "Relative foil-fluid velocity estimation and forecasting for cyclorotor wave energy conversion," in *Proc. IEEE OCEANS 2025 Conf.*, Brest, France, 2025.

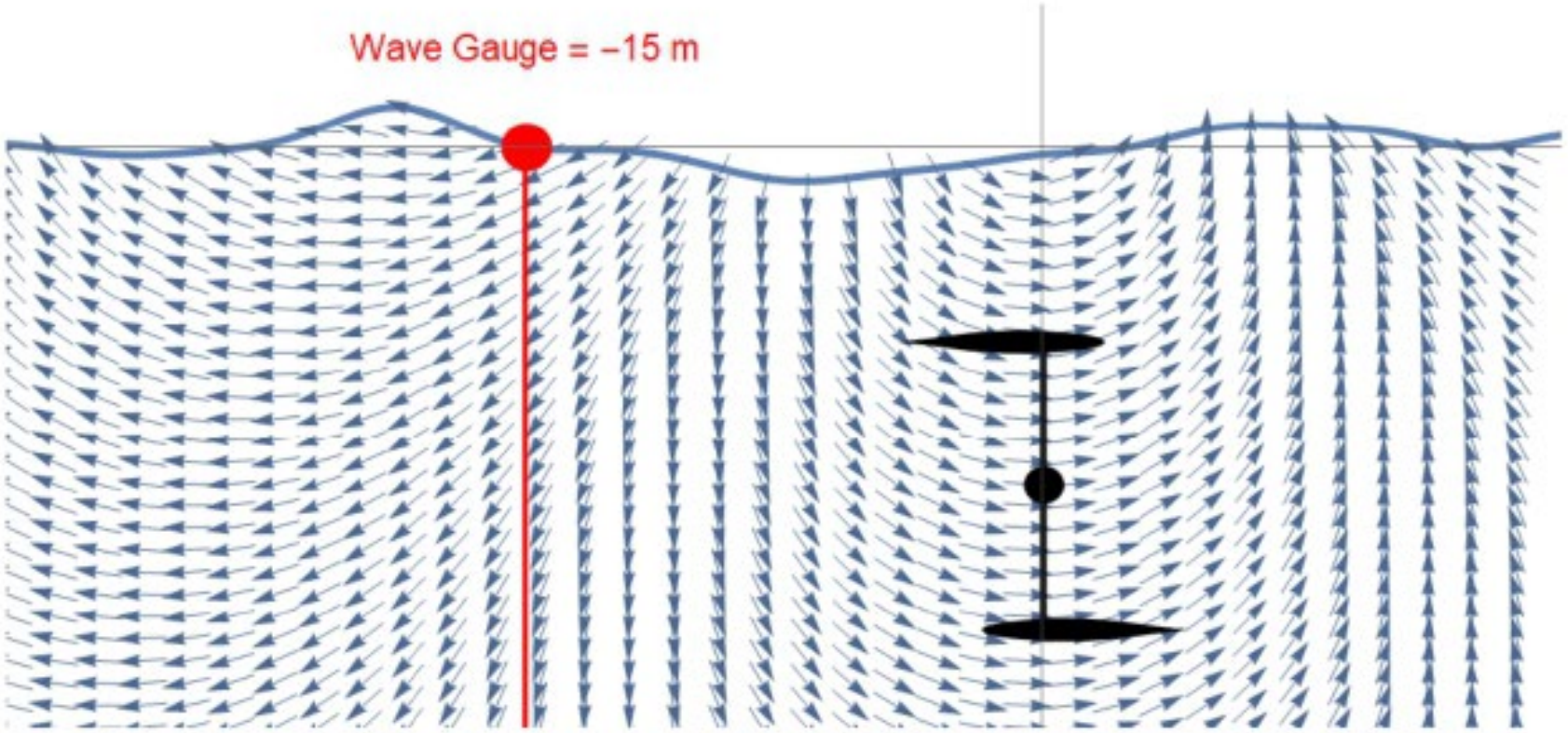

Figure 9: Irregular wave-induced fluid velocity vector field, cyclorotor WEC, and location of the up-wave free surface elevation gauge.

Predictor

- The training data is generated in MATLAB using simulations of a cyclorotor WEC similar to the one suggested by the Atargis Energy Corporation, with the same parameters as before.

Predictor

- The training data is generated in MATLAB using simulations of a cyclorotor WEC similar to the one suggested by the Atargis Energy Corporation, with the same parameters as before.

- A panchromatic sea state with peak period $T_p = 10$s and significant wave height $H_s = 2$m is considered.

Predictor

- The training data is generated in MATLAB using simulations of a cyclorotor WEC similar to the one suggested by the Atargis Energy Corporation, with the same parameters as before.

- A panchromatic sea state with peak period $T_p = 10$s and significant wave height $H_s = 2$m is considered.

- The data are normalized and divided into training, validation and testing sets.

Predictor

- The training data is generated in MATLAB using simulations of a cyclorotor WEC similar to the one suggested by the Atargis Energy Corporation, with the same parameters as before.

- A panchromatic sea state with peak period $T_p = 10$s and significant wave height $H_s = 2$m is considered.

- The data are normalized and divided into training, validation and testing sets.

- The LSTM RNN model is trained and tested in PYTHON, using TensorFlow and Keras libraries.

Predictor

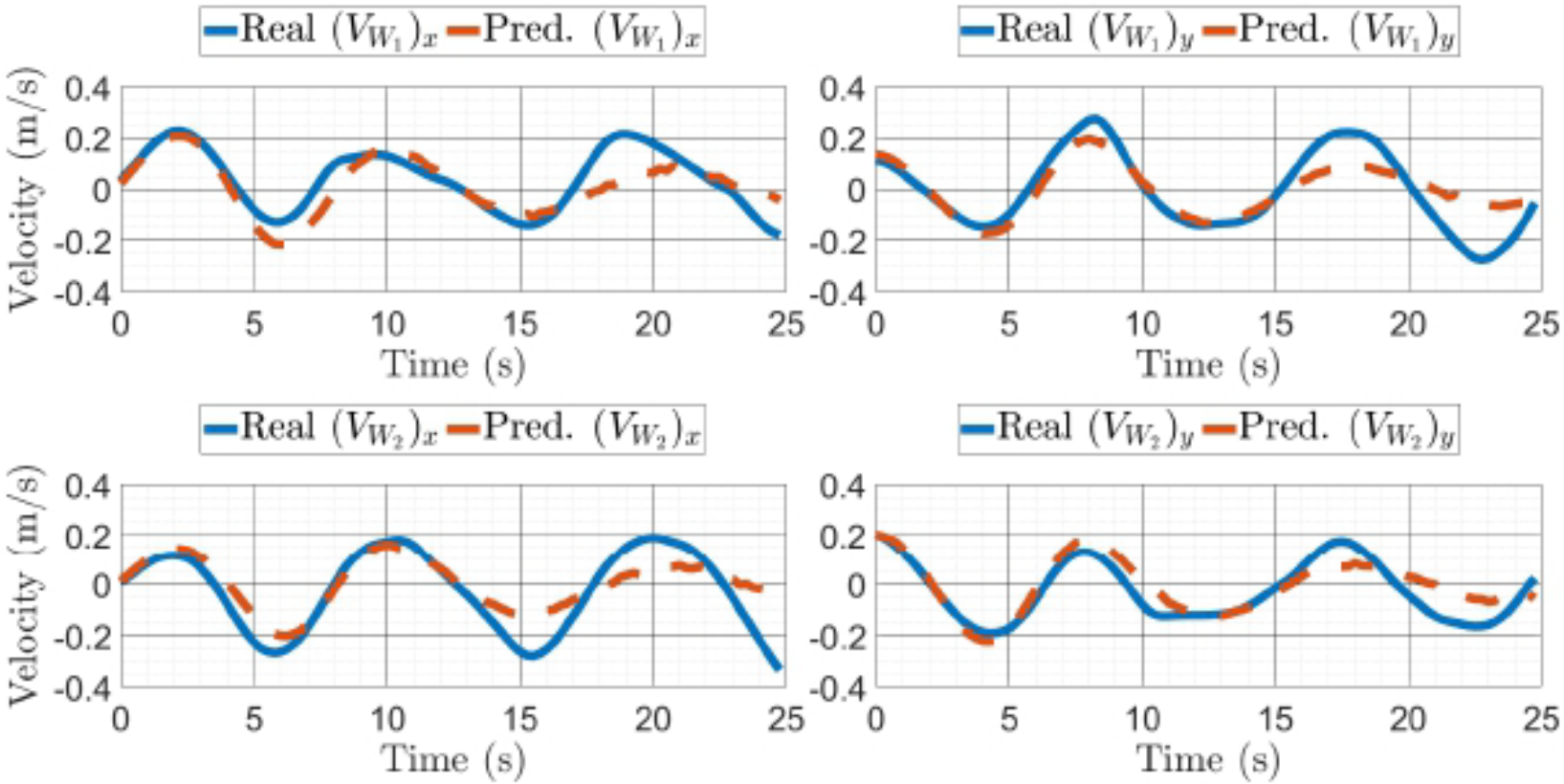

Figure 10: Comparison between the actual and predicted x and y components of the wave-induced fluid velocity vector $\mathbf{V_W}$ for both hydrofoils.

Similar approach to the one proposed in [8].

NMPC formulation

$$\min_{\dot{\theta}(t),\,\gamma_1(t),\,\gamma_2(t)} \quad J = \frac{1}{T_0}\int_0^{T_0} \left(-\mathcal{T}_{PTO}(t)\dot{\theta}(t) + \mu\,\Delta\mathcal{T}^2_{\mathrm{PTO}}(t)\right)\,dt,$$

$$\text{s.t.} \quad (0.2H_s + 0.6)\,\omega_p \;\leq\; \dot{\theta}(t) \;\leq\; (0.2H_s + 1)\,\omega_p,$$

$$-15^\circ \;\leq\; \{\gamma_1(t),\,\gamma_2(t)\} \;\leq\; 15^\circ.$$

[8] I. Stasinopoulos, A. Ermakov, and J. V. Ringwood, "Nonlinear model predictive control strategies for a cyclorotor wave energy device," in *Proc. 23rd Eur. Control Conf. (ECC)*, Thessaloniki, Greece, 2025.

- A cyclorotor WEC similar to the one suggested by the Atargis Energy Corporation, with the same parameters as before, is considered.

Nonlinear MPC

- A cyclorotor WEC similar to the one suggested by the Atargis Energy Corporation, with the same parameters as before, is considered.

- Implementation with MATLAB MPC Toolbox.

Nonlinear MPC

- A cyclorotor WEC similar to the one suggested by the Atargis Energy Corporation, with the same parameters as before, is considered.

- Implementation with MATLAB MPC Toolbox.

- Optimization problem solved with MATLAB `fmincon` solver.

Nonlinear MPC

- A cyclorotor WEC similar to the one suggested by the Atargis Energy Corporation, with the same parameters as before, is considered.

- Implementation with MATLAB MPC Toolbox.

- Optimization problem solved with MATLAB `fmincon` solver.

- MATLAB script communicates with the PYTHON-based predictor using the `pyenv` interface.

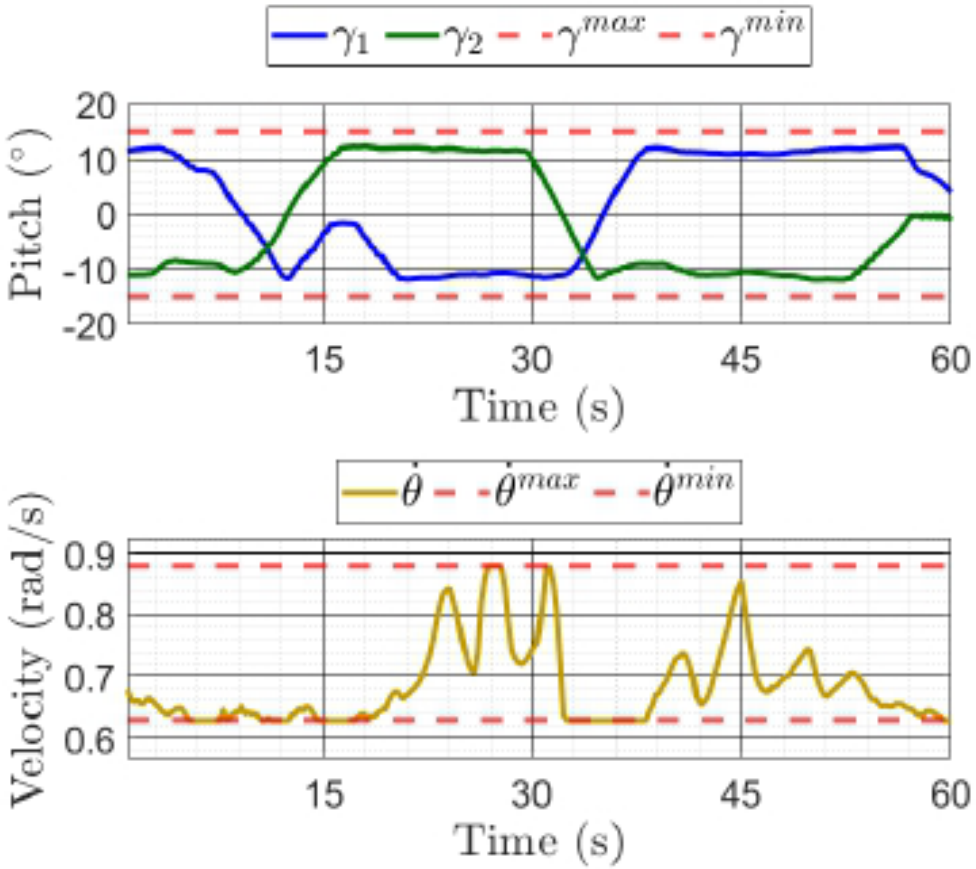

Figure 11: Pitch angles and angular velocity time-series with active upper and lower constraints over a one-minute interval, under the proposed realistic control, for a representative irregular sea state, with $T_p = 10$ s and $H_s = 2$ m.

Results

Results

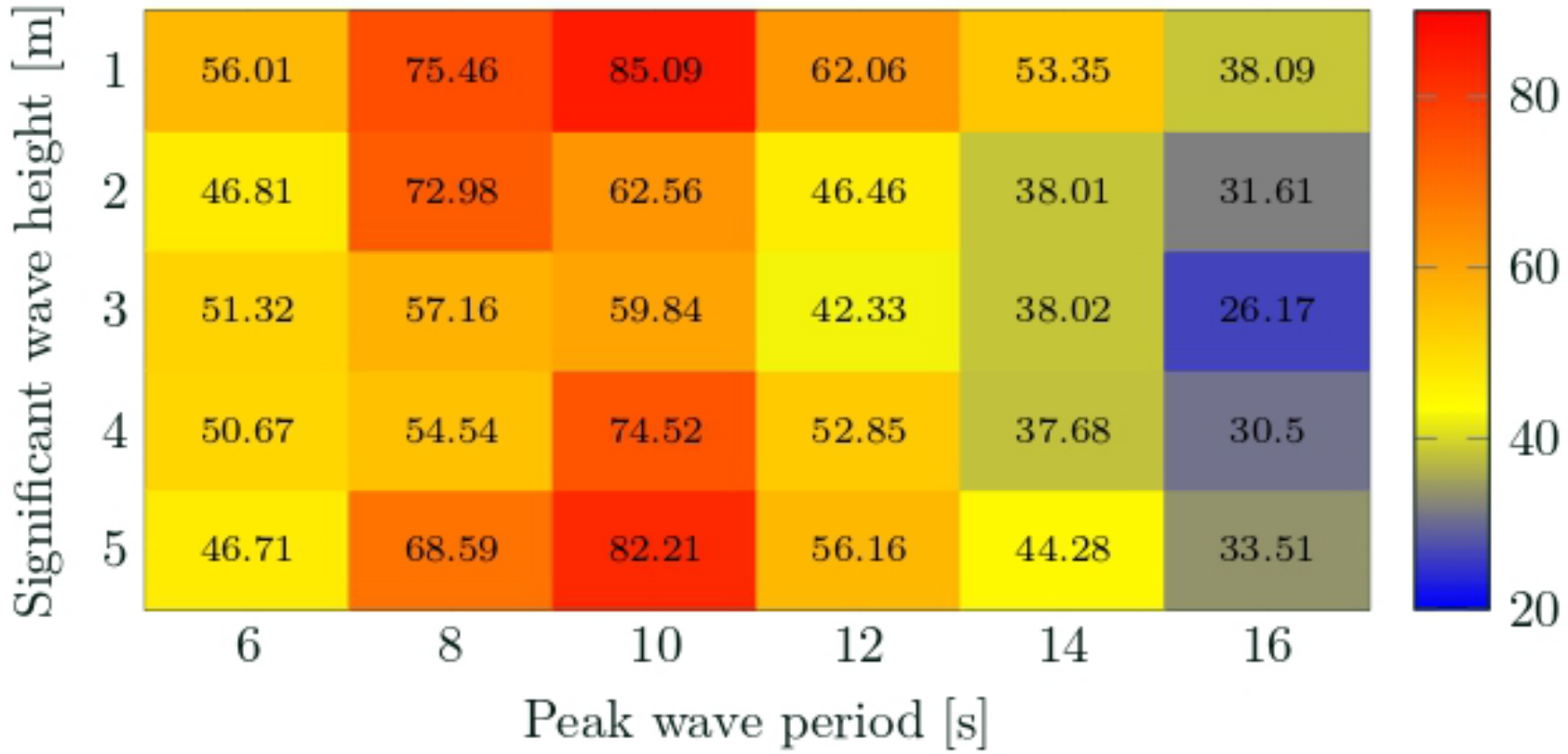

Mechanical power generation in CWR [%] across sea states, assuming ideal estimation and perfect knowledge of the relative foil-fluid velocity.

Results

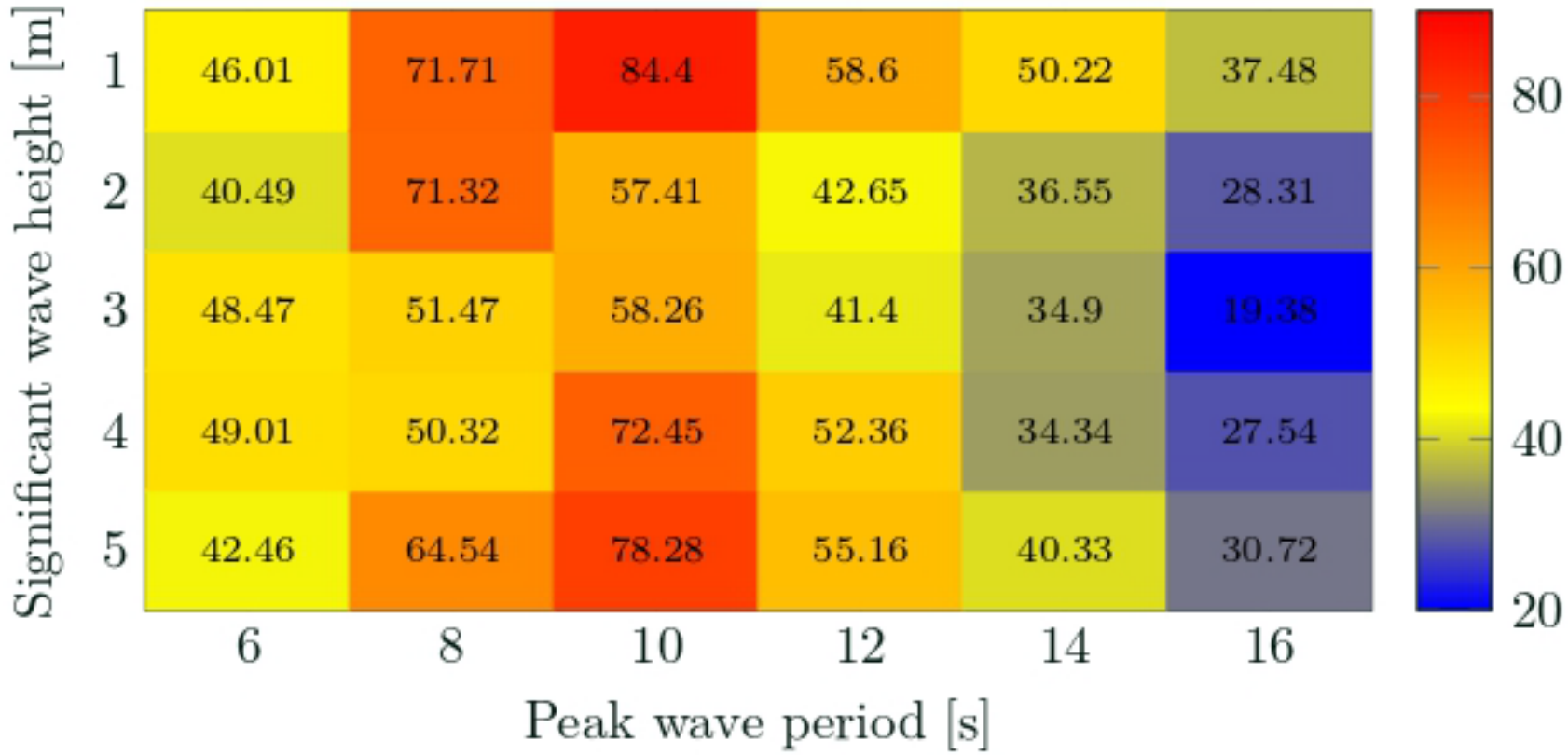

Mechanical power generation in CWR [%] across sea states, incorporating estimator and predictor of the relative foil-fluid velocity.

Results

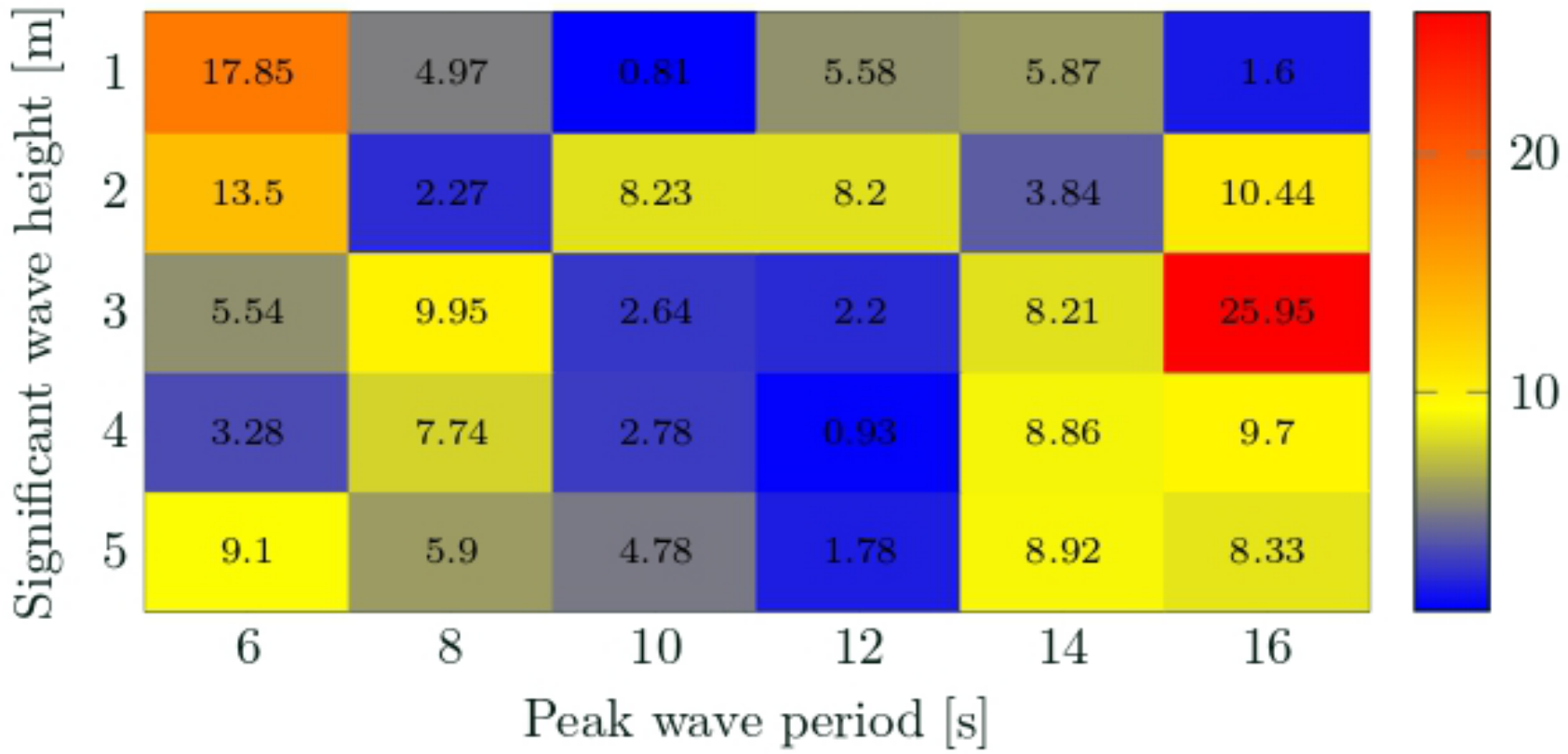

Relative difference in CWR [%] across sea states between the idealised and the realistic case.

Table 2: Idealized and realistic total annual mechanical energy production for different locations in MWh per hydrofoil span meter.

Wave climate location	Idealized control	Realistic control
Humboldt Bay	101.57 MWh/m	95.98 MWh/m
Bay of Biscay	74.21 MWh/m	70.27 MWh/m

- Total annual mechanical energy is calculated based on wave data obtained from ERA5 for the year 2024.
- The overall loss due to estimation and prediction inaccuracies is just **under 6%** for both regions.

Conclusions and discussion

Conclusions and discussion

- The energy capture losses due to estimation and prediction errors are quantified, and found to be within acceptable limits.

Conclusions and discussion

- The energy capture losses due to estimation and prediction errors are quantified, and found to be within acceptable limits.

- For the first time, realistic estimates of annual mechanical power production are obtained for two key locations proposed for potential cyclorotor WEC installation: The Humboldt Bay and the Bay of Biscay.

Conclusions and discussion

- The energy capture losses due to estimation and prediction errors are quantified, and found to be within acceptable limits.

- For the first time, realistic estimates of annual mechanical power production are obtained for two key locations proposed for potential cyclorotor WEC installation: The Humboldt Bay and the Bay of Biscay.

- At present, the implementation of the proposed control system does not yet achieve real-time performance.

Conclusions and discussion

- The energy capture losses due to estimation and prediction errors are quantified, and found to be within acceptable limits.

- For the first time, realistic estimates of annual mechanical power production are obtained for two key locations proposed for potential cyclorotor WEC installation: The Humboldt Bay and the Bay of Biscay.

- At present, the implementation of the proposed control system does not yet achieve real-time performance.

- No pitch actuation and PTO system are included, which could account for pitch position and torque errors, respectively.

Thank you!

Happy to answer your questions

"*Realistic energy-maximising control of cyclorotor wave energy converters using estimator, predictor, and nonlinear MPC.*"

Ilias Stasinopoulos[1], A. Ermakov[1], J.V. Ringwood[1].

Acknowledgements: This work was supported in part by a research grant from Taighde Éireann (Research Ireland) and the Sustainable Energy Authority of Ireland under the Pathway Programme (22/PATH-S/10793).

Ilias Stasinopoulos
ilias.stasinopoulos.2025@mumail.ie
coer.maynoothuniversity.ie

Supplementary material: Model

The wake-induced velocity field is modeled using a complex potential formulation [8]:

$$\mathcal{F}(z,t) = \frac{\Gamma(t)}{2\pi \mathrm{i}} \log\left[\frac{z - c(t)}{z - \tilde{c}(t)}\right] - \frac{2\mathrm{i}\sqrt{g}}{\pi} \int_0^t \frac{\Gamma(\tau)}{\sqrt{\mathrm{i}(z - \tilde{c}(\tau))}} D\left[\frac{\sqrt{g}(t-\tau)}{2\sqrt{\mathrm{i}(z - \tilde{c}(\tau))}}\right] d\tau,$$

where $z = x + \mathrm{i}y$ denotes the complex spatial coordinate, $c(\tau) = x(\tau) + \mathrm{i}y(\tau)$ is the complex position of the hydrofoil at an earlier time τ, Γ is the intensity of circulation of the point vortex, and $D(x)$ is the Dawson function, defined as:

$$D(x) = e^{-x^2} \int_0^x e^{y^2} dy.$$

[8] A. Ermakov, F. Thiebaut, G. S. Payne, and J. V. Ringwood, "Validation of a control-oriented point vortex model for a cyclorotor-based wave energy device," *J. Fluids Struct.*, vol. 119, p. 103875, 2023.

Supplementary material: Model

The velocity field from the complex potential is extracted as:

$$V_H = \frac{\partial \mathcal{F}(z,t)}{\partial z} = (V_H)_x - \mathrm{i}\,(V_H)_y\,.$$

The total induced velocity on hydrofoil i is calculated as:

$$V_{H_i} = V_{HM_j} + V_{HW_i} + V_{HW_j}\,,$$

where V_{HM} is the instantaneous radiation from the moving hydrofoil and V_{HW} captures the trailing wake left by the hydrofoil.

Supplementary material: Estimator

System state vector: $x = [\dot{\theta}, (V_{W_1})_x, (V_{W_1})_y, (V_{W_2})_x, (V_{W_2})_y]$
Observation vector: $h = [\dot{\theta}, F_{T_1}, F_{R_1}, F_{T_2}, F_{R_2}]$
Control input vector: $u = [\gamma_1, \gamma_2, \mathcal{T}_{PTO}]$
Then, the model function and measurement function are given by:

$$\dot{x}(t) = f(x(t), u(t)) + w(t),$$
$$z = h(x(t), u(t)) + v(t),$$

respectively, where the random vectors $w(t) \sim N(0, Q(t))$ and $v(t) \sim N(0, R(t))$ represent the process and measurement noise respectively.

Supplementary material: Estimator

Now, the state transition matrix and the observation matrix can be found as the Jacobians:

$$F(t) = \left.\frac{\partial f}{\partial x}\right|_{x(t),u(t)}, H(t) = \left.\frac{\partial h}{\partial x}\right|_{x(t),u(t)}.$$

Finally, the predict and update phase of the EKF can be given by:

$$\dot{\hat{x}}(t) = f\left(\hat{x}(t, u(t))\right) + K(t)(z(t) - h(\hat{x}(t))),$$

where:

$$K(t) = P(t)H(t)^T R(t)^{-1},$$
$$\dot{P}(t) = F(t)P(t) + P(t)F(t)^T - K(t)H(t)P(t) + Q(t).$$

with $P(t)$ the state error covariance matrix amd $K(t)$ the Kalman gain.

Supplementary material: Predictor

- Model architecture: Two bidirectional LSTM layers with 192 and 128 units, respectively, and one fully connected (dense) layer.

- Model training: Adam optimizer with a learning rate of 0.0083 and a batch size of 64.

- The time length of the input sequences is 12.5 s and the time length of the output sequences is 25 s.

- All hyperparameters optimized using Bayesian optimization via the Optuna library.

Supplementary material: NMPC

Table 3: NMPC tuning parameters [9]

NMPC parameters		
Sampling interval T_s	0.25	[s]
Prediction horizon t_p	7.5	[s]
Weighting factor μ	10^{-5}	

[9] I. Stasinopoulos, A. Ermakov, and J. V. Ringwood, "Nonlinear model predictive control strategies for a cyclorotor wave energy device," in *Proc. 23rd Eur. Control Conf. (ECC)*, Thessaloniki, Greece, 2025.

Supplementary material: Real-time?

- The combined estimator-predictor-NMPC execution time is approximately 14.3 s, which significantly exceeds the adopted control timestep of 0.25 s.
- Software, rather than algorithmic, limitations.
- High computational cost associated with the combined execution of the estimator and NMPC in MATLAB, together with the data-driven predictor in Python.

- A fully compiled implementation in C/C++ is expected to reduce computation time significantly.
- The numerical solutions, obtained using the proposed control approach, can be used to train a neural network for the development of a physics-informed neural network based control strategy.
- Main focus for now: **Demonstrate the potential of the proposed realistic energy-maximising control for cyclorotor WECs.**